Jurnal Polimesin
Department of Mechanical Engineering
State Polytechnic of Lhokseumawe
http://e-jurnal.pnl.ac.id/polimesin
e-ISSN : 2549-1999 No. : 2 Month : April
p-ISSN : 1693-5462 Volume : 23 Year : 2025

Processing dates: received on 2025-01-03, reviewed on 2025-02-28, accepted on 2025-04-30 and online availability on 2025-04-30

# Enhanced structural and thermal properties of oil palm frond fiber-derived nanocellulose using chemical and mechanical treatments for eco-friendly composites

**Randis[1],*, F. Gapsari[2]**
[1]Departement of Mechanical Engineering, Balikpapan State Polytechnic, Balikpapan 76126, Indonesia
[2]Departement of Mechanical Engineering, University of Brawijaya, Malang 65145, Indonesia
*Corresponding Author: randis@poltekba.ac.id

**Abstract**

This study investigates the extraction and characterization of Cellulose Nanofibrils (CNFs) from Oil Palm Frond Fibers (OPFFs) using a combined chemical and mechanical treatment approach. Alkali treatment and bleaching effectively removed non-cellulosic components, increasing the Crystallinity Index (CI) from 58.75% in untreated OPFFs to 73.09% in Chemically Treated Microfibrillated cellulose (CMFs). Subsequent ultrafine grinding further enhanced the CI to 81.93%, demonstrating high purity and improved structural integrity. Thermogravimetric Analysis (TGA) revealed enhanced thermal stability, with the maximum degradation temperature rising from 286°C in OPFFs to 339°C in CNFs. X-ray Diffraction (XRD) analysis confirmed the retention of the cellulose of crystalline structure after all treatments. The novelty of this study lies in the systematic valorization of oil palm frond fibers, an abundant agricultural waste in Indonesia, through an integrated chemical-mechanical process to produce high-performance nanocellulose. These findings demonstrated that OPF-derived CNFs possess superior structural and thermal properties, making them strong candidates for reinforcing eco-friendly polymer composites in sustainable material applications.

**Keywords:**
Cellulose nanofibrils, oil palm frond fibers, chemical-mechanical treatment, crystallinity index, thermal stability

## 1 Introduction

Indonesia's position as the world's largest palm oil and palm oil producer is not without significant environmental consequences. The expansion of oil palm plantations, which covered 15.4 million hectares [1], has resulted in substantial agricultural waste, particularly solid biomass. Among the various types of waste generated, Oil Palm Fronds (OPFs) represent the largest solid waste source, environmental degradation, and economic challenges. Historically, the disposal of OPFs has been problematic, with standard practices including burning, which releases pollutants [2], or allowing them to accumulate on plantation grounds, while accumulation disrupts ecosystems [3]. The increasing volume of OPF waste presents a unique opportunity to convert this abundant resource into value-added products, particularly through the extraction of nanocellulose. Nanocellulose, known for its exceptional properties such as high surface area, high aspect ratio, and superior mechanical strength, has shown great potential as a reinforcement material in composite applications [4], [5]. Utilizing OPF-derived nanocellulose could address environmental and economic concerns, providing a sustainable solution for waste management while contributing to developing high-performance, eco-friendly bio-composites.

Despite the promising potential of nanocellulose, the challenge lies in effectively isolating and processing cellulose nanofibers from OPFs to achieve the desired properties for high-performance applications. Current methods for nanocellulose extraction from various lignocellulosic sources have yielded promising results; despite promising results from current methods, the potential of chemical-mechanical treatments to optimize OPF-derived nanocellulose remains underexplored, particularly in achieving high purity and enhanced properties. The complexity of OPF's lignocellulosic structure, consisting of cellulose, hemicellulose, and lignin, necessitates an optimized extraction process to achieve high purity and desirable nanofiber characteristics. This study proposes a solution by employing a chemical-mechanical treatment to isolate cellulose nanofibers from OPFs. The combination of alkaline pretreatment and ultrafine grinding aims to effectively break down the lignocellulosic matrix and yield high-quality nanofibers with enhanced thermal stability and crystallinity. However, while numerous studies have explored nanocellulose extraction from other agricultural residues such as pineapple leaf fibers and sugarcane bagasse, the potential of Oil Palm Frond Fibers (OPFs) remains underexplored, particularly regarding the optimization of chemical-mechanical treatments to maximize crystallinity and thermal stability. This method is expected to produce nanofibers that are well-suited for reinforcing biopolymer composites, offering a pathway to more sustainable materials.

The use of nanocellulose as a reinforcement in polymer composites has been extensively studied, demonstrating significant improvements in mechanical and thermal properties. The inclusion of nanocellulose in ethylene-acrylic acid copolymer composites led to substantial increases in tensile strength and modulus, highlighting the material's effectiveness in enhancing composite performance [6]. Similarly, nanocellulose-reinforced epoxy composites achieved impressive modulus values, which are indicative of effective reinforcement [7]. The effectiveness of nanocellulose as a reinforcing agent is attributed to its unique structural characteristics, such as a high aspect ratio and large surface area, which facilitate strong interactions with the polymer matrix [8]. These interactions are critical for ensuring efficient stress transfer and enhancing the mechanical performance of the composite. Moreover, the thermal properties of nanocellulose composites are significantly improved due to the enhanced interfacial interactions, as influenced by the glass transition temperature of the polymer matrix [9]. In addition to its mechanical and thermal advantages, nanocellulose also offers environmental benefits, particularly biodegradability. Nanocellulose exhibits superior biodegradability compared to traditional fillers, making it an ideal choice for eco-friendly composite applications. The combination of these properties underscores the potential of OPF-derived nanocellulose as a valuable material for sustainable composite production.

Despite extensive research on nanocellulose derived from various biomass sources, studies focusing on extracting and characterizing cellulose nanofibers from OPFs using chemical-mechanical methods remain scarce. Most studies have focused on other lignocellulosic sources, leaving a gap in understanding how OPF-derived nanocellulose compares its structural and functional properties. Furthermore, the environmental and economic potential of utilizing OPF waste for nanocellulose production has not been fully explored, particularly in sustainable bio-composite development.

This study aims to address these gaps by employing a combination of alkali treatment, bleaching, and ultrafine grinding to enhance the quality of OPF-derived nanocellulose. The study aims to explore OPFs as an underutilized biomass resource, particularly in Indonesia, and their potential to be transformed into high-value nanocellulose for eco-friendly biopolymer composites. By

investigating the effects of chemical-mechanical treatment on the morphology, crystallinity, and thermal stability of the isolated nanofibers, this study seeks to provide new insights into applying OPF-derived nanocellulose as a reinforcement material for sustainable composite production. Nevertheless, the existing body of research often lacks comprehensive investigations into the structural and thermal enhancements achievable through combined chemical and mechanical methods specifically applied to OPFs. This creates a critical research gap that this study intends to address.

## 2 Methods

### 2.1 Materials

Twenty-year-old oil palms (Elaeis guineensis Jacq) were sourced from a plantation in Kuaro Subdistrict, Paser Regency, East Kalimantan, Indonesia. The cellulose fibers were extracted from the frond sheath, the section closest to the stem, as it is the most suitable part for fiber extraction [10][11]. The fronds were cleaned of spines and outer skin using a knife, chopped into 30-cm pieces, and washed under running water. The pieces were soaked in room-temperature water for 2–3 days to ease fiber separation.

The chemical composition of OPFs is primarily characterized by cellulose (34.89%), hemicellulose (27.14%), and lignin (19.87%), which are major constituents of lignocellulosic biomass [12]. In addition to these primary components, OPFs contain a relatively high ash content (14.3%), which affects biomass combustion efficiency and ash residue characteristics [13]. The presence of extractives, including soluble sugars, proteins, and minerals, further influences the chemical behavior of OPFs in various applications, such as material science and agriculture [14]. The fibers were then oven-dried at 70°C until the water content was reduced to 9–10%. They were subsequently cut into smaller pieces and ground with a blender to achieve uniform particle sizes capable of passing through a 60-mesh sieve. Chemical processing utilized analytical-grade distilled water, sodium hydroxide (99% NaOH, Merck), and hydrogen peroxide (30% $H_2O_2$, Merck Millipore®), procured from Sigma-Aldrich®.

### 2.2 The Isolation of cellulose and CNFs from OPF

#### 2.2.1 Isolation of cellulose

The chemical treatment of the fibers involved maceration and bleaching techniques to remove lignin and hemicellulose from the unprocessed fibers. The cellulose extraction process of the OPFFs employed an initial alkaline treatment where the fibers were macerated in 9% natrium hydroxide (NaOH) with a fiber to solution ratio of 1:25. Then, they were heated at 70°C for 1 h and then rinsed with distilled water to get a neutral pH of 7.0. Next, they were oven-dried at 105°C until the water content reached 9-10%. The stage was followed by a bleaching process, which was repeated twice, in which the alkaline-treated fibers were heated in a 25% hydrogen peroxide ($H_2O_2$) solution at 70°C for one hour to produce pure white cellulose. Then it was cleaned with double distilled water to reach a neutral pH and oven-dried under the same conditions as during the maceration process.

#### 2.2.2 Preparation of CNFs

Through the prior chemical treatment, a fiber identified as cellulose microfibers (CMFs) was formed. Next, a mechanical treatment was done on the CMFs using an ultrafine grinding technique. First, the procedure was conducted by adding 1 g of CNFs to a 1% concentration. It was followed by sonification employing the Sonic Ruptor 400, which operated at a frequency of 40 kHz and had an output power of 80% during 60 min, with a tool tip diameter of 13 mm. The treatment was conducted at room temperature, resulting in the transformation of the suspension. The suspension was processed twice through the ultrafine grinding machine of MKCA6-3 (Masuko Sangyo Co. Ltd., Japan), which was set with an open gap of 10 µm for 1 min to disperse the material. The outcome was a fiber solution containing 1% cellulose and 99% water, cellulose nanofibers (CNFs).

The ultrafine grinding was performed under fixed operational settings: the grinding disc gap was set to −30 µm, the rotational speed was maintained at 1500 rpm, and the material was processed for approximately 1 minute per pass. Each sample was subjected to 40 passes through the grinder to ensure consistent fibrillation. The pressure was indirectly regulated throughout the grinding process by adjusting the disc gap and monitoring the motor load to maintain a stable mechanical shear force without overheating the material. No additional external pressure was applied. The following nano fibrillation procedure was carried out in contact mode with a rotating speed of 1500 rpm and a gap between two dics set to -30 m, and was repeated 40 times. The detailed process of extraction and isolation to get the CNFs from OPF is illustrated in Fig. 1.

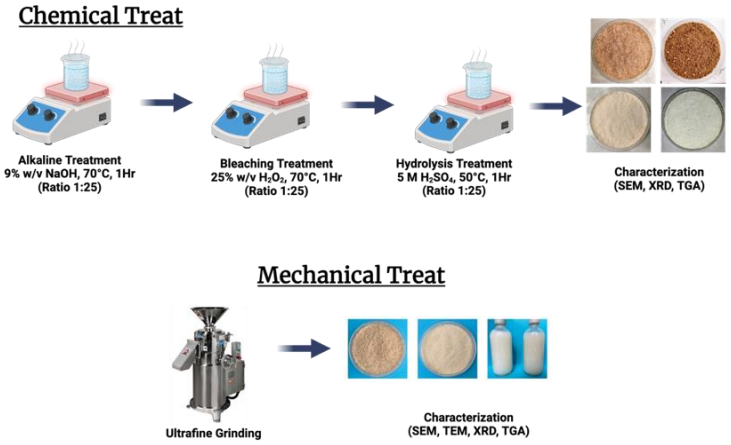


Fig. 1. Detailed process of extraction and isolation used to obtain CNFs from OPF

### 2.3 Characterization

To ensure the reproducibility and reliability of the results, all treatments and characterizations were performed in triplicate. The obtained results were averaged, and standard deviations were calculated where appropriate to confirm data consistency.

The morphological, structural, and thermal properties of the untreated and treated fibers were evaluated using several analytical techniques as described below.

#### 2.3.1 SEM analysis

The surface morphology of OPFFs, CMFs, and CNFs was studied with the SEM (FEI Inspect S-50) at 20 kV acceleration voltage and 8 mA probe current. Prior to the analysis, the microfibers were evenly placed over conductive tape and subjected to a 60-second gold sputtering process to improve conductivity and reduce overcharging, resulting in improved image clarity.

TEM analysis was conducted on nanocellulose following mechanical treatment, including ultrafine grinding and ultrasonication. The surface morphology of cellulose nanofibers (CNFs) was examined using a JEM-1400 Transmission Electron Microscope (JEOL Ltd., Japan) operating at a voltage of 100 kV. The cellulose nanofiber suspension was placed onto a carbon film supported by a copper grid and then dried. The dried samples were observed under TEM at room temperature.

#### 2.3.2 XRD analysis

An XRD analysis was performed on the fiber before and after the treatment using an X'Pert PRO PANalytical diffractometer (Philips Analytical, Almelo, Netherlands) equipped with Cu Kα radiation. Measurements were made at 40 kV with a filament current of 30 mA at diffraction angles (2θ) ranging from 5º to 80° and a scanning speed of 4°/min. The Crystallinity Index (CI) was determined based on the Segal method [15].

$$\mathrm{CrI}\ (\%) = \left[\frac{I_{002} - I_{am}}{I_{002}}\right] \times 100 \qquad (1)$$

The CI was calculated from the maximum intensity in the (002) field (I002, 2θ = 22 - 23°), indicating the crystal region, and the minimum intensity between the (101) and (002) fields (Iam, 2θ = 18°), corresponding to the amorphous region. This comprehensive analysis allows a detailed assessment of the crystalline and amorphous phases in the fiber.

### 2.3.3 Thermal degradation analysis

The thermal properties and stability of both the untreated and treated fibers were evaluated using a thermogravimetric analyzer (Thermogravimetric Analysis (TGA)-1 Metler Toledo) under atmospheric nitrogen conditions. The analysis involved a heating rate of 10°C/min and a temperature range of 30-600°C, with a nitrogen flow rate maintained at 50 mL/min and a sample weight of about 5 mg.

## 3 Results and Discussion

### 3.1 Characterization of the fibers

#### 3.1.1 Visual changes in the colour and structure of the OPF

Fig. 2 illustrates the progressive visual and structural changes in Oil Palm Frond (OPF) fibers subjected to chemical and mechanical treatments. Raw OPF Fibers (Image a) displays the untreated fibers exhibit a light brown hue and a coarse texture, characteristic of lignocellulosic material in its natural state. After Alkali Treatment (Image b) Indicate the fibers darken to a deeper brown color, indicating the removal of lignin as it degrades and dissolves. The texture becomes finer, with small clumps appearing due to partial fiber separation. After Bleaching (Image c), the fibers transition to a bright white color, reflecting further removal of non-cellulosic components such as residual lignin. The structure becomes finer and more uniform. Finally, after Ultrafine Grinding (Image d) the fibers transform into a thick, gel-like white suspension, signaling significant changes in both color and consistency. This state indicates successful nano-fibrillation, with fibers reduced to nanoscale dimensions.


Fig. 2. Visual and structural transformation of OPF fibers after various treatments

These observations align with existing literature, where similar color and structural changes have been reported during the chemical and mechanical treatment of lignocellulosic fibers. The darkening after alkali treatment corresponds to lignin removal, consistent with findings in windmill palm fibers [16]. Bleaching enhances fiber whiteness, as reported in other studies [17]. Finally, the gel-like consistency after ultrafine grinding reflects a reduction in fiber size and an increase in surface area, similar to results observed in mechanically treated lignocellulosic fibers [18].

The visual and structural changes demonstrate the effectiveness of the sequential treatment steps in refining OPF fibers. Each stage—alkali treatment, bleaching, and ultrafine grinding—contributes to purifying the fibers and enhancing their properties for advanced applications. The high degree of nano fibrillation achieved after ultrafine grinding is particularly significant, as it is essential for strong interfacial bonding in composite materials.

These findings emphasize the potential of OPF-derived nanocellulose as an eco-friendly and high-performance reinforcement material for bio composites. The methodical transformation process optimizes the fibers' mechanical and thermal properties and highlights their applicability as a sustainable alternative in material science, aligning with goals for environmental sustainability and resource efficiency.

#### 3.1.2 SEM and TEM analysis

Fig. 3 presents SEM and TEM images illustrating the morphological changes in OPF fibers at various chemical and mechanical treatment stages. To clearly show the parts described in the figure, each subfigure (a–d) is explained in detail to highlight the structural modifications observed.

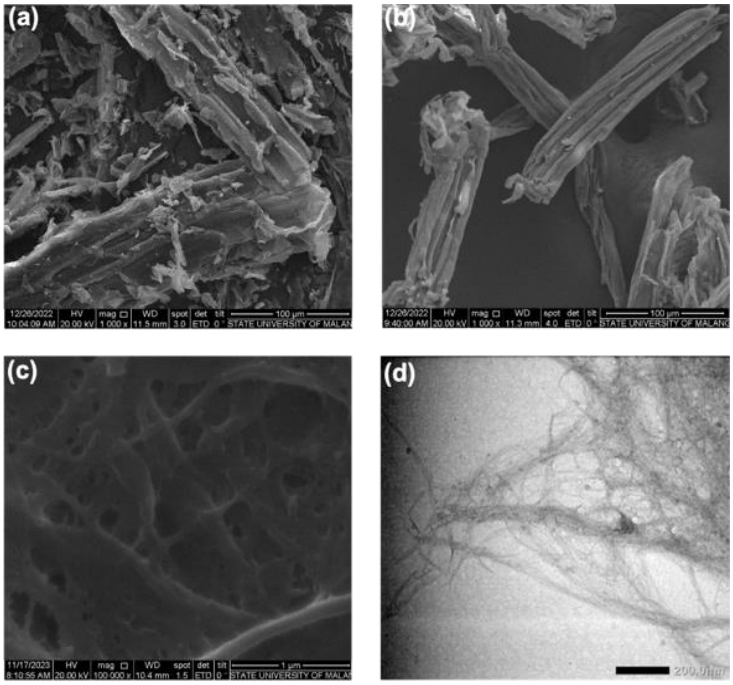


Fig. 3. SEM micrograph of OPFFs (a); chemically treated (CMFs) (b); and SEM and TEM of CNFs (c-d)

In Fig. 3(a), the untreated OPFFs exhibit a coarse and irregular surface, with fiber bundles tightly bound by non-cellulosic components such as lignin and hemicellulose. The rough and compact structure of the untreated fibers indicates the presence of natural plant polymers that reinforce the fiber matrix, making them resistant to mechanical separation.

Fig. 3(b) shows the OPF fibers after undergoing alkali treatment and bleaching, leading to a significant reduction in fiber diameter from 86.35 ± 1.24 µm to 36.31 ± 1.45 µm. This size reduction is accompanied by a cleaner and more fibrillated fiber surface, indicating the successful removal of lignin and hemicellulose. The more open structure allows for greater accessibility to the cellulose component, which is crucial for further mechanical processing.

In Fig. 3(c), Cellulose Nanofibrils (CNFs) is shown using SEM imaging, highlighting the structural transformation achieved through ultrafine grinding. The image reveals a significant reduction in fiber dimensions, where the fiber bundles appear more separated and individual nanofibrils are distinctly visible. This observation suggests that the ultrafine grinding process effectively breaks down the larger fiber structures into nanoscale fibrils. The increased

fibrillation enhances surface area and accessibility, which is crucial for improving the material's mechanical properties. Furthermore, the well-dispersed nanofibrils promote better interaction with polymer matrices, thereby enhancing their reinforcing capabilities in composite applications.

Fig. 3(d) presents the final transformation of OPF fibers into CNFs after ultrafine grinding, using TEM imaging. At this stage, the fibers exhibit diameters ranging between 10 and 100 nm, forming a highly entangled network of fine fibrils. The formation of nanoscale fibrils significantly increases the fiber surface area, which enhances its interaction with polymer matrices in composite applications. The fine structure observed at this stage confirms the effectiveness of the ultrafine grinding process in breaking down the cellulose into nanoscale elements.

The morphological changes observed in the SEM and TEM images are consistent with findings in the literature regarding the effects of chemical and mechanical treatments on lignocellulosic fibers. The significant reduction in fiber diameter following alkali treatment and bleaching, as seen in Figs. 3(b) and (c), aligns with previous studies that reported similar outcomes, where the removal of lignin and hemicellulose led to a more refined and fibrillated fiber structure [19]–[21]. The transition to nanoscale fibrils after ultrafine grinding, depicted in Fig. 3(d), is also supported by the work of Khalil et al. (2014), who observed that mechanical processing effectively reduces fiber dimensions and increases surface area, enhancing the fibers' applicability in composite materials [22].

The results demonstrated in Fig. 3 have critical implications for the potential application of OPF-derived nanocellulose in various industrial sectors, particularly in the production of bio composites. The reduction in fiber diameter and the production of CNFs highlight the effectiveness of the applied treatments in improving the mechanical properties of the fibers. The cleaner and more fibrillated structure observed in the treated fibers suggests enhanced compatibility with polymer matrices, which is crucial for the development of high-performance composite materials. Furthermore, the nanoscale dimensions achieved through ultrafine grinding indicate a significant potential for these fibers to be used in applications requiring high surface area and strong mechanical properties.

The reduction in fiber diameter, as observed in Figs 3(b) and (c), is inversely correlated with an increase in fiber strength. This relationship is well-documented in the literature, where smaller fiber dimensions are associated with higher aspect ratios, leading to better compatibility and bonding with polymer matrices in composite applications [23]. The enhanced strength and compatibility of the smaller diameter fibers make them ideal candidates for reinforcing materials in composite structures, contributing to the overall mechanical performance of the final product.

The chemical and mechanical treatments applied to the OPF fibers affected their morphology and significantly impacted their crystallinity and thermal stability. The increase in crystallinity observed in the CNFs, as inferred from their morphology in Fig. 3(d), is crucial for applications that require materials with superior mechanical and thermal properties. The enhanced thermal stability resulting from these treatments makes the nanocellulose fibers particularly suitable for high-temperature applications in various industrial sectors, further expanding their potential uses. These improvements underscore the value of combining chemical and mechanical treatments to optimize the properties of lignocellulosic fibers for advanced material applications.

Although detailed histogram analysis of the fiber diameter distribution was not conducted, measuring average diameters and standard deviations across multiple samples ($n \geq 30$) provides a reliable quantitative representation of the morphological changes. The substantial decrease in average fiber diameter, from $86.35 \pm 1.24$ μm in untreated OPFFs to $36.31 \pm 1.45$ μm after chemical treatment, and finally to nanoscale dimensions (10–100 nm) observed in TEM images, clearly demonstrates the effectiveness of the chemical-mechanical treatment approach. Future studies are encouraged to include histogram-based statistical analyses to strengthen the quantitative understanding of fiber diameter distribution further.

### 3.1.3 X-Ray Diffraction (XRD) analysis

Fig. 4 shows the XRD patterns for OPFFs, Chemically-treated Micro Fibrillated Cellulose (CMFs), and CNFs. The diffraction peaks at 2θ angles of 18°, 22.6°, and 34.5° correspond to the crystallographic planes (101), (002), and (040) of cellulose I, respectively, indicating the presence of cellulose I structure in all samples. The CI values increase progressively from 58.75% for OPFFs, to 73.09% for CMFs, and to 81.93% for CNFs, reflecting the effectiveness of both chemical and mechanical treatments in enhancing the crystallinity of the cellulose.

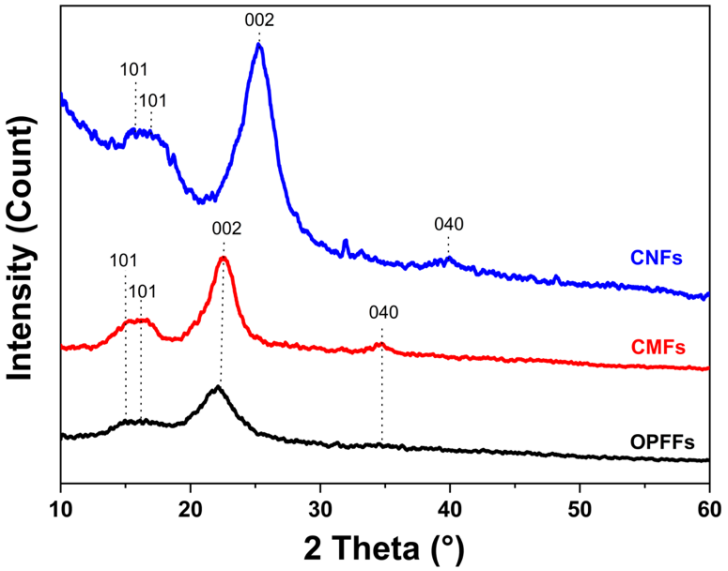


Fig. 4. The XRD curve of the OPFFs, CMFs, and CNFs

Compared to other natural sources of nanocellulose reported in the literature, the CI of CNFs obtained from OPF fibers (81.93%) is relatively high. In contrast, nanocellulose derived from Barangan banana fibers shows lower crystallinity, ranging from 54% to 57.3% [24]. Similarly, Agave americana fibers exhibit a CI of 70.4% [25], while Agave cantala and Oil Palm Empty Fruit Bunch (OPEFB) fibers display crystallinity indices of 78.2% and 71.27%, respectively [26][27]. These comparisons indicate that the chemical-mechanical treatment approach applied to OPF fibers effectively produces CNFs with crystallinity levels comparable to those obtained from traditional high-cellulose sources such as cotton, while surpassing several other agricultural residues. This highlights the potential of OPFs as a promising and sustainable source for high-performance nanocellulose production.

The increase in CI observed in Fig. 4 is consistent with previous studies that have shown similar effects of chemical and mechanical treatments on lignocellulosic fibers. The initial CI of 58.75% for untreated OPFFs is within the range expected for raw plant fibers, where the amorphous components, such as lignin and hemicellulose, contribute to a lower crystallinity. The increase to 73.09% for CMFs following alkali and bleaching treatments is aligned with findings of previous research [28], which indicate that the removal of amorphous components leads to higher crystallinity. The further increase to 81.93% for CNFs after ultrafine grinding supports the results reported by Gapsari et al. (2022) [29], where mechanical processing led to a substantial increase in CI, emphasizing the role of such treatments in enhancing cellulose purity and crystalline structure.

The progressive increase in crystallinity from OPFFs to CNFs, as demonstrated in Fig. 3, is significant for applications that require materials with high mechanical strength and thermal stability. Higher crystallinity in cellulose is directly related to improved mechanical properties, such as tensile strength and modulus, making the CNFs particularly suitable for reinforcing composite materials.

Moreover, the maintenance of the cellulose I structure across all treatments ensures that the inherent desirable properties of the cellulose are preserved, which is crucial for the integrity and performance of the final materials in various industrial applications, including bio composites and nanomaterials.

The notable increase in CI following chemical treatments (from OPFFs to CMFs) can be attributed to removing amorphous regions within the cellulose, particularly lignin and hemicellulose, which contribute to lower crystallinity. This finding is supported by other studies that have demonstrated similar increases in CI following the elimination of non-cellulosic components [19]. The effective removal of these components through alkali and bleaching treatments not only enhances the crystallinity but also improves the overall purity and quality of the cellulose, making it more suitable for high-performance applications.

While the increase in CI following ultrafine grinding observed in this study aligns with some previous reports, other studies have noted a decrease in CI following mechanical treatments. This discrepancy could be attributed to differences in treatment protocols, such as the combination of ultrafine grinding and ultrasonication, which has been shown to disrupt crystalline regions and reduce crystallinity [30]. The variability in CI outcomes highlights the importance of optimizing mechanical processing parameters to achieve the desired balance between crystallinity and other material properties. The higher CI observed in this study suggests that the chosen mechanical treatments effectively preserved and enhanced the crystalline structure of the cellulose, making the resulting CNFs highly suitable for applications requiring superior mechanical performance.

### 3.1.4 Thermal stability

Figs 5a and 5b present the Thermogravimetric (TG) and Derivative Thermogravimetric (DTG) analysis of OPFFs, CMFs, and CNFs, highlighting their thermal degradation behavior across temperature ranges.

Table 1 presents a summary of the thermal stability data, including the initial degradation temperature, main degradation temperature, final decomposition temperature, and weight loss at each stage of degradation.

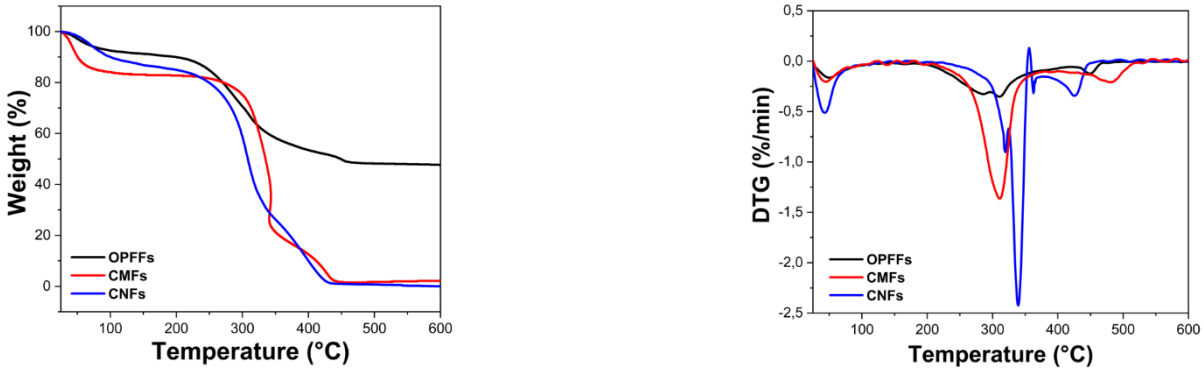


(a) (b)

Fig. 5. a. TGA b. DTG of OPFFs, CMFs and CNFs

Table 1. OPFFs, CMFs and CNFs

| Sample | Initial degradation Temp (°C) | Main Degradation Temp Range (°C) | Final Degradation Temp (°C) | Weight Loss (%) |
|---|---|---|---|---|
| OPFFs | 65°C | 286°C | 420°C | 65% |
| CMFs | 80°C | 311°C | 450°C | 90% |
| CNFs | 88°C | 339°C | 500°C | 95% |

The table clearly shows that the initial degradation temperatures for all samples occur at around 50°C due to moisture evaporation. The main degradation temperatures, however, exhibit a progressive increase, with OPFFs degrading at 286°C, CMFs at 311°C, and CNFs at 339°C. This trend reflects the increasing crystallinity and purity of CNFs due to the applied treatments, enhancing their thermal resistance. The final decomposition temperature remains consistent at approximately 550°C across all samples, but the weight loss data indicate significant differences. OPFFs leave a higher residue due to their lignin and mineral content, while CMFs and CNFs display lower residual formation, confirming the successful removal of non-cellulosic impurities through chemical treatments.

Moisture Evaporation (50–100°C): At this stage, all samples exhibit an initial weight loss due to the evaporation of adsorbed water and hydrogen-bonded moisture. OPFFs show a higher moisture content compared to processed fibers, indicating the presence of non-cellulosic components, which can retain water. The reduction in moisture content in CMFs and CNFs confirms that the chemical and mechanical treatments effectively eliminated hydrophilic impurities. These findings align with previous studies that demonstrate how crystallinity influences the interaction between cellulose and moisture [31]–[34].

Cellulose Degradation (210–350°C): Significant weight loss occurs in this range due to polymer breakdown, hemicellulose degradation, and glycosidic bond cleavage [35]. The DTGmax values are observed at 286°C for OPFFs, 311°C for CMFs, and 339°C for CNFs. OPFFs degrade at 286°C, showing lower thermal stability due to hemicellulose and lignin. CMFs degrade at 311°C, demonstrating enhanced stability after removing non-cellulosic components. CNFs degrade at 339°C, exhibiting the highest thermal stability, which is attributed to increased crystallinity and purity of cellulose nanofibrils. The significant increase in thermal stability from OPFFs to CNFs confirms that chemical-mechanical treatments effectively enhance the material's resistance to decomposition, making them more suitable for high-temperature applications [36][37]. These results align with the increased crystallinity and purity observed in treated fibers, validating their potential for high-performance bio composite applications.

Final Decomposition Stage (400–550°C): In the final decomposition stage, around 400 and 550°C, ash and residual waste formation is evident. OPFFs leave a high residue due to their higher lignin and mineral content, which do not fully degrade at lower temperatures. In contrast, CMFs and CNFs exhibit lower residual formation, confirming that the chemical treatments successfully removed most non-cellulosic impurities [38]. The findings align with XRD results, which show an increase in the CI from 58.75% in OPFFs to 73.09% in CMFs and 81.93% in CNFs. The correlation between increased crystallinity and thermal stability further validates the effectiveness of the chemical and mechanical treatments in refining OPF-derived nanocellulose for high-performance applications. The sharper DTG peaks of treated fibers indicate the successful elimination of non-cellulosic materials, confirming their potential for use in thermally stable bio composites and supporting sustainable material development.

The observed thermal degradation of OPFFs, CMFs, and CNFs can be attributed to typical decomposition mechanisms of lignocellulosic materials. The weight loss at 50–100°C initially corresponds to the evaporation of free and bound water molecules. In the main degradation phase (210–350°C), significant weight loss

is associated with the depolymerization of cellulose chains and the breakdown of glycosidic linkages, leading to the release of volatile products such as levoglucosan, carbon dioxide, and water. The cleavage of intermolecular hydrogen bonds within the cellulose structure also contributes to this thermal instability. Finally, at higher temperatures (400–550°C), the carbonaceous residues undergo further decomposition, forming a residual char. The reduced residue observed in CMFs and CNFs compared to OPFFs is attributed to the effective removal of lignin and hemicellulose, which typically degrade at lower temperatures and leave behind more char. These degradation pathways reflect the enhanced thermal resilience and purity of the treated fibers, confirming their suitability for applications requiring improved thermal stability.

## 4 Conclusion

This study successfully demonstrated that a combination of alkali treatment, bleaching, and ultrafine grinding effectively extracted and enhanced the quality of CNFs from OPFFs. The treatments significantly improved the CI (from 58.75% to 81.93%) and thermal stability (maximum degradation temperature increasing from 286°C to 339°C), confirming the enhanced structural integrity and purity of the resulting CNFs.

The findings highlight the significant potential of OPF-derived CNFs as reinforcement materials in eco-friendly bio composites, particularly for high-performance industrial applications such as lightweight automotive parts, packaging materials, and biodegradable composites. These applications not only offer mechanical advantages but also contribute to the advancement of sustainable material technologies.

Future research should focus on scaling up the production process to industrial levels, optimizing the dispersion of CNFs in polymer matrices, and evaluating the long-term durability and performance of CNF-reinforced composites under real-world service conditions.

## References


[1] BPS, “Luas Tanaman Perkebunan Menurut Provinsi (Ribu Hektar), 2023.”

[2] O. Folahan, A.-W. Taiwo, A. Ghazali, A. Khalil, and A. Hassan, “Isolation and Characterization of Microcrystalline Cellulose from Oil Palm Fronds using Chemomechanical Process,” *Wood Fiber Sci.*, vol. 48, no. 4, pp. 1–11, 2016.

[3] E. Saputra, H. Sugesti, B. A. Prawiranegara, Y. Aziz, A. Fadli, and O. Muraza, “Waste materials from palm oil plant as exploratory catalysts for FAME biodiesel production,” *Appl. Nanosci.*, vol. 12, no. 12, pp. 3703–3719, 2022, doi: 10.1007/s13204-021-02185-9.

[4] I. Mawardi, N. Nurdin, F. Fakiza, A. Jannifar, H. Razak, and R. Putra Jaya, “Performance of blockboard using particle composite bagasse waste as core layer materials,” *Compos. Adv. Mater.*, vol. 33, pp. 1–11, 2024, doi: 10.1177/26349833241232996.

[5] I. Hasanuddin, I. Mawardi, N. Nurdin, and R. P. Jaya, “Evaluation of properties of hybrid laminated composites with different fiber layers based on Coir/Al2O3 reinforced composites for structural application,” *Results Eng.*, vol. 17, no. February, p. 100948, 2023, doi: 10.1016/j.rineng.2023.100948.

[6] V. Abhijit, T. Johannes, K. Sahlin-Sjövold, R. Mikael, and A. Boldizar, “Melt processing of ethylene-acrylic acid copolymer composites reinforced with nanocellulose,” *Polym. Eng. Sci.*, vol. 60, no. 5, pp. 956–967, 2020, doi: 10.1002/pen.25351.

[7] L. Yue, F. Liu, S. Mekala, A. Patel, R. A. Gross, and I. Manas-Zloczower, “High performance biobased epoxy nanocomposite reinforced with a bacterial cellulose nanofiber network,” *ACS Sustain. Chem. Eng.*, vol. 7, no. 6, pp. 5986–5992, 2019, doi: 10.1021/acssuschemeng.8b06073.

[8] N. Masruchin, “Nanocellulose, The Origin of Natural Reinforcement in Advanced Biocomposites,” *J. Fibers Polym. Compos.*, vol. 2, no. 1, pp. 64–66, 2023, doi: 10.55043/jfpc.v2i1.82.

[9] T. Kaldéus, A. Träger, L. A. Berglund, E. Malmström, and G. Lo Re, “Molecular engineering of the cellulose-poly (caprolactone) bio-nanocomposite interface by reactive amphiphilic copolymer nanoparticles,” *ACS Nano*, vol. 13, no. 6, pp. 6409–6420, 2019.

[10] M. S. Mat Rasat, R. Wahab, Z. Abdul Kari, A. A. Mohd Yunus, J. Moktar, and S. F. Mhd. Ramle, “Strength properties of bio-composite lumbers from lignocelluloses of oil palm fronds agricultural residues,” *Int. J. Adv. Sci. Eng. Inf. Technol.*, vol. 3, no. 3, p. 199, 2013, doi: 10.18517/ijaseit.3.3.320.

[11] M. Rasat., R. Wahab, O. Sulaiman, A. Moktar, Janshah. Mohamed, and I. Tabet, A. T. Khalid, “Properties of Composite Boards From Oil Palm,” *BioResources*, vol. 6, no. 4, pp. 4389–4403, 2011, doi: 10.15376/biores.6.4.4389-4403.

[12] S. Maulina and F. A. F. Sinaga, “The opportunities of oil palm fronds become a commercial liquid smoke,” in *Materials Science Forum*, Trans Tech Publ, 2019, pp. 159–166, doi: 10.4028/www.scientific.net/MSF.948.159.

[13] O. Chavalparit, M. Ongwandee, and K. Trangkaprasith, “Production of pelletized fuel from biodiesel-production wastes: oil palm fronds and crude glycerin,” *Eng. J.*, vol. 17, no. 4, pp. 61–70, 2013, doi: 10.4186/ej.2013.17.4.61.

[14] P. Romyen, Y. Pianroj, T. Punvichai, S. Karrila, A. Chotikhun, and S. Jumrat, “Utilization of Used Bleaching Clay in Pellet Fuel Production with Torrefied Oil Palm Fronds.,” *BioResources*, vol. 18, no. 4, 2023, doi: 10.15376/biores.18.4.6986-7002

[15] L. Segal, J. J. Creely, A. E. Martin, and C. M. Conrad, “An Empirical Method for Estimating the Degree of Crystallinity of Native Cellulose Using the X-Ray Diffractometer,” *Text. Res. J.*, vol. 29, no. 10, pp. 786–794, 1959, doi: 10.1177/004051755902901003.

[16] C. Chen, W. Yin, G. Chen, G. Sun, and G. Wang, “Effects of biodegradation on the structure and properties of windmill palm (Trachycarpus fortunei) fibers using different chemical treatments,” *Materials (Basel).*, vol. 10, no. 5, p. 514, 2017, doi: 10.3390/ma10050514.

[17] S. Gnanasekaran, S. N. N. Muslih, J. H. Shariffuddin, and N. Nordin, “Effect of steam and bleaching treatment on the characteristics of pineapple leaves fibre derived cellulose,” *Pertanika J. Sci. Technol*, vol. 28, no. S2, pp. 135–148, 2020, doi: 10.47836/pjst.28.S2.11.

[18] G. Chen *et al.*, “Influence of chemical composition of windmill palm fibre on crystallinity after alkali peroxide bleaching by grey model,” *J. Eng. Fiber. Fabr.*, vol. 14, p. 1558925019883451, 2019, doi: 10.1177/1558925019883451.

[19] R. Randis, D. B. Darmadi, F. Gapsari, A. As, and A. Sonief, “Isolation and characterization of microcrystalline cellulose from oil palm fronds biomass using consecutive chemical treatments,” *Case Stud. Chem. Environ. Eng.*, vol. 9, no. December 2023, p. 100616, 2024, doi: 10.1016/j.cscee.2024.100616.

[20] N. Ndwandwa, F. Ayaa, S. A. Iwarere, M. O. Daramola, and J. B. Kirabira, “Extraction and characterization of cellulose

nanofibers from yellow thatching grass (Hyparrhenia filipendula) straws via acid hydrolysis," *Waste and Biomass Valorization*, vol. 14, no. 8, pp. 2599–2608, 2023, doi: 10.21203/rs.3.rs-1819436/v1.

[21] R. Jagadeesan, I. Suyambulingam, R. Somasundaram, D. Divakaran, and S. Siengchin, "Isolation and characterization of novel microcellulose from Sesamum indicum agro - industrial residual waste oil cake : conversion of biowaste to wealth approach," *Biomass Convers. Biorefinery*, pp. 4427–4441, 2023, doi: 10.1007/s13399-022-03690-9.

[22] H. P. S. A. Khalil *et al.*, "Production and modification of nanofibrillated cellulose using various mechanical processes : A review," *Carbohydr. Polym.*, vol. 99, pp. 649–665, 2014, doi: 10.1016/j.carbpol.2013.08.069.

[23] A. Poulose *et al.*, "Nanocellulose: a fundamental material for science and technology applications," *Molecules*, vol. 27, no. 22, p. 8032, 2022, doi: 10.3390/molecules27228032.

[24] R. Ratna, N. Arahman, A. A. Munawar, and S. Aprilia, "Extraction, isolation, and characterization of nanocrystalline cellulose from barangan banana (musa acuminata L.) peduncles waste," *Indones. J. Chem.*, vol. 23, no. 1, pp. 73–89, 2023, doi: 10.22146/ijc.74718.

[25] P. Krishnadev, K. S. Subramanian, G. J. Janavi, S. Ganapathy, and A. Lakshmanan, "Synthesis and characterization of nano-fibrillated cellulose derived from green Agave americana L. fiber," *BioResources*, vol. 15, no. 2, p. 2442, 2020, doi: 10.15376/biores.15.2.2442-2458

[26] F. Yudhanto, J. Jamasri, H. S. B. Rochardjo, and A. Kusumaatmaja, "Experimental study of polyvinyl alcohol nanocomposite film reinforced by cellulose nanofibers from agave cantala," *Int. J. Eng.*, vol. 34, no. 4, pp. 987–998, 2021.

[27] P. Amanda, S. Nabila, N. Qonita, R. S. Ningrum, and N. Masruchin, "The properties of OPEFB cellulose nanofibrils produced by a different mode of ultrafine grinding," in *IOP Conference Series: Earth and Environmental Science*, IOP Publishing, 2021, p. 12016, doi: 10.1088/1755-1315/891/1/012016.

[28] N. F. S. M. Azani, M. K. M. Haafiz, A. Zahari, S. Poinsignon, N. Brosse, and M. H. Hussin, "Preparation and characterizations of oil palm fronds cellulose nanocrystal (OPF-CNC) as reinforcing filler in epoxy-Zn rich coating for mild steel corrosion protection," *Int. J. Biol. Macromol.*, vol. 153, pp. 385–398, 2020, doi: 10.1016/j.ijbiomac.2020.03.020.

[29] A. Andoko, F. Gapsari, K. Diharjo, S. M R, and S. Siengchin, "Isolation of microcellulose from timoho fiber using the process of delinigfication and maceration: Evaluation of physical, chemical, structural, and thermal properties," *Int. J. Biol. Macromol.*, vol. 224, no. October 2022, pp. 48–54, 2022, doi: 10.1016/j.ijbiomac.2022.10.225.

[30] S. N. Mousavi, N. Nazarnezhad, G. Asadpour, S. K. Ramamoorthy, and A. Zamani, "Ultrafine friction grinding of lignin for development of starch biocomposite films," *Polymers (Basel).*, vol. 13, no. 12, p. 2024, 2021, doi: 10.3390/polym13122024.

[31] R. M. Sheltami, I. Abdullah, I. Ahmad, A. Dufresne, and H. Kargarzadeh, "Extraction of cellulose nanocrystals from mengkuang leaves ( Pandanus tectorius )," *Carbohydr. Polym.*, vol. 88, no. 2, pp. 772–779, 2012, doi: 10.1016/j.carbpol.2012.01.062.

[32] H. Ren *et al.*, "Preparation of microcrystalline cellulose from agricultural residues and their application as polylactic acid/microcrystalline cellulose composite films for the preservation of Lanzhou lily," *Int. J. Biol. Macromol.*, vol. 227, no. December 2022, pp. 827–838, 2023, doi: 10.1016/j.ijbiomac.2022.12.198.

[33] M. Mahardika, H. Abral, A. Kasim, S. Arief, and M. Asrofi, "Production of nanocellulose from pineapple leaf fibers via high-shear homogenization and ultrasonication," *Fibers*, vol. 6, no. 2, pp. 1–12, 2018, doi: 10.3390/fib6020028.

[34] M. Ioelovich, "Application of thermochemical method to determine the crystallinity degree of cellulose materials," *Appl. Sci.*, vol. 13, no. 4, p. 2387, 2023, doi: 10.3390/app13042387.

[35] A. Ahmed and A. Qayoum, "Investigation on the thermal degradation, moisture absorption characteristics and antibacterial behavior of natural insulation materials," *Mater. Renew. Sustain. Energy*, vol. 10, no. 1, pp. 1–10, 2021, doi: 10.1007/s40243-021-00188-8.

[36] A. F. Tarchoun, D. Trache, T. M. Klapötke, M. Derradji, and W. Bessa, "Ecofriendly isolation and characterization of microcrystalline cellulose from giant reed using various acidic media," *Cellulose*, vol. 26, pp. 7635–7651, 2019, doi: 10.1007/s10570-019-02672-x.

[37] A. A. Oun and J.-W. Rhim, "Isolation of cellulose nanocrystals from grain straws and their use for the preparation of carboxymethyl cellulose-based nanocomposite films," *Carbohydr. Polym.*, vol. 150, pp. 187–200, 2016, doi: 10.1016/j.carbpol.2016.05.020.

[38] A. Sinclair, L. Jiang, D. Bajwa, S. Bajwa, S. Tangpong, and X. Wang, "Cellulose nanofibers produced from various agricultural residues and their reinforcement effects in polymer nanocomposites," *J. Appl. Polym. Sci.*, vol. 135, no. 21, p. 46304, 2018, doi: 10.1002/app.46304.